scientific reports

Check for updates

OPEN

Efficient control strategy for electric furnace temperature regulation using quadratic interpolation optimization

Serdar Ekinci[1], Davut Izci[1,2], Veysel Gider[3], Laith Abualigah[4,5], Mohit Bajaj[6,7,8]✉ & Ievgen Zaitsev[9,10]✉

Electric furnaces play an important role in many industrial processes where precise temperature control is essential to ensure production efficiency and product quality. Traditional proportional-integral-derivative (PID) controllers and their modified versions are commonly used to maintain temperature stability by reacting quickly to deviations. In this study, the real PID plus second-order derivative (RPIDD^2) controller is introduced for the first time for industrial temperature control applications, which is a novel alternative that has not yet been investigated in the literature. To ensure optimal performance, the parameters of the RPIDD^2 controller are optimized using metaheuristic algorithms, including the flood optimization algorithm (FLA), reptile search algorithm (RSA), particle swarm optimization (PSO) and differential evolution (DE). A new approach is proposed which combines the quadratic interpolation optimization (QIO) algorithm with the RPIDD^2 controller, taking advantage of the fast convergence, low computational cost and high accuracy of QIO. Comparative analyses between QIO-RPIDD^2, FLA-RPIDD^2, RSA-RPIDD^2, PSO-RPIDD^2 and DE-RPIDD^2 controller are performed by evaluating performance metrics such as transient and frequency response. The results show that QIO-RPIDD^2 achieves superior performance, adapts quickly to different reference temperatures and performs excellently on key performance indicators. These results make the proposed QIO-RPIDD^2 controller a promising solution for industrial temperature control and contribute to more efficient and adaptive optimization techniques.

Keywords Quadratic interpolation optimization, Real PID plus second-order derivative controller, Temperature control, Time response, Frequency response

Electric furnaces are the most commonly used furnaces in the industrial sector. They are used in various fields such as metal processing, ceramic production, chemical reactions, glass processing, medical sterilization and laboratory experiments. These furnaces play a crucial role in temperature control processes that require high precision by converting electrical energy into heat. The operation and control of temperature is a factor that requires very precise, accurate and fast control in technical and industrial applications. Accurate temperature control ensures that the product maintains the desired properties in the production process. If the temperature is not controlled to an appropriate value, the physical properties of the material in question may change or deteriorate. Therefore, it is very important and necessary to maximize the precision, speed and accuracy of temperature control to achieve the best performance. For this reason, many approaches to temperature control of electric furnaces have been developed and applied. In general, techniques such as manual control, thermostatic

[1]Department of Computer Engineering, Batman University, 72100 Batman, Turkey. [2]Applied Science Research Center, Applied Science Private University, Amman 11931, Jordan. [3]Distance Education Application and Researcher Center, Batman University, Batman, Turkey. [4]Computer Science Department, Al al-Bayt University, Mafraq 25113, Jordan. [5]Jadara Research Center, Jadara University, Irbid 21110, Jordan. [6]Department of Electrical Engineering, Graphic Era (Deemed to be University), Dehradun 248002, India. [7]College of Engineering, University of Business and Technology, 21448 Jeddah, Saudi Arabia. [8]Graphic Era Hill University, Dehradun 248002, India. [9]Department of Theoretical Electrical Engineering and Diagnostics of Electrical Equipment, Institute of Electrodynamics, National Academy of Sciences of Ukraine, Beresteyskiy, 56, Kyiv-57, Kyiv 03680, Ukraine. [10]Center for Information-Analytical and Technical Support of Nuclear Power Facilities Monitoring, National Academy of Sciences of Ukraine, Akademika Palladina Avenue, 34-A, Kyiv, Ukraine. ✉email: thebestbajaj@gmail.com; zaitsev@i.ua

control, proportional-integral-derivative (PID) control, proportional (P) control, sliding mode control (SMC), and internal model control (IMC) are used to precisely control the temperature in electric furnaces[1,2]. Among these, the PID controller is the most commonly used and most powerful. Accordingly, PID controllers stand out from the various control approaches developed for temperature control.

Although the PID controller is still the controller of choice, the refinement and development of control strategies is critical to the sustainability and cost-effectiveness of the overall performance of industrial processes based on electric furnaces. Conventional PID controllers are often inadequate for non-linear systems, so advanced controller designs are required. Therefore, in addition to PID, there are various advanced controllers such as PID acceleration (PIDA), fractional order PID (FOPID) and real PID plus second order derivative (RPIDD^2)[3–7]. Nowadays, there are many techniques for tuning PID and its variants. Researchers have a challenge in calibrating PID controllers due to the non-linear characteristics of electric furnace systems. Moreover, the parameters of the system could shift over the course of time. Utilizing control techniques that are both intelligent and adaptive is therefore a more advantageous choice when it comes to fine-tuning PID controllers. Even among controllers with comparable architectures, different optimization methodologies exist. These methods are advised for optimizing the settings of controllers used in regulating the temperature of electric furnaces[8–17]. Techniques for enhancing controller parameters encompass fuzzy logic (FL)[18,19], neural networks[20], whale optimization algorithm (WOA)[2], genetic algorithm (GA)[1], Ziegler-Nichols method[21], and particle swarm optimization (PSO)[22] utilizing model predictive control. These methods are proposed to provide more precise and adaptive tuning of PID controllers, especially in complex systems.

Lopez et al.[23] attempted to regulate the temperature profile of the SiC sample by modelling and controlling the SF60 solar furnace. Strategies such as PI controller, feedforward control and PI-based feedback linearization control were developed and validated on the real system. Sheng et al.[24] conducted a study aimed at improving the efficiency and quality of grain drying by developing a multi-channel hot air oven with biomass recirculation. The simulation and test results showed that adaptive fuzzy PID control provided better dynamic response and accuracy of ± 3 °C compared to conventional PID control. Surus et al.[25] presented the use of a gain-timing (G-S) PID controller for precise temperature control in semiconductor crystal annealing and growth processes. The simulation and experimental results showed that the G-S enhanced system improves the performance compared to the standard PID controller by shortening the temperature rise time. Wang et al.[26] presented a control framework that aims to reduce pollutant emissions by optimizing the furnace temperature (FT) in municipal solid waste incineration processes. With ISNA-PID control and PSO optimization, 19.93% less NOx emissions and 6.99% less CO_2 emissions were achieved. Lopez et al.[27] presented a cascade control system that combines industrial PID with a model-independent controller to control complex heating processes. Simulation and experiments show that the proposed system outperforms conventional cascade controllers in terms of accuracy and adaptability. Chen et al.[28] redesigned the relationship between temperature (TIC) and flow (FIC) controllers in a multi-slope structure to reduce temperature load disturbances in reheat furnaces. The experimental results show that the proposed method improves the speed and stability of temperature response by reducing the mean square error by 33.76% and the standard deviation by 22.44%. Beccaro et al.[29] compared PI and fuzzy PI algorithms for the control of a three-zone open tube furnace in semiconductor manufacturing. The fuzzy PI controller showed superior performance at 900 °C, kept the temperature variation below ± 1.06 °C, and provided a fast-settling time. Zhang et al.[30] proposed a dual fuzzy-PID control method for fast temperature control of a MEMS TGA. The simulation and test results showed that the method provided faster response and less overshoot compared to conventional PID controllers.

In analyzing some studies using the above techniques, some researchers used fuzzy logic to tune the PID controller to control the temperature of the electric furnace and treated it as a first-order system[31]. The researchers concluded that the proposed control method is superior to the conventional PID controller. The researchers concluded that the proposed control method is superior to the conventional PID controller. On the other hand, Liu et al.[32] proposed an online tuned fractional-order PID control algorithm with fuzzy rules to achieve higher accuracy, robustness and dynamic performance in industrial temperature control systems. In another study[33], a PSO-PID controller optimized by the PSO algorithm and a split-range control strategy were used to control the temperature in an ethanol fermentation process. They show that their proposed method provides high control performance in temperature control and more effective error control than other methods. Jamil et al.[5] investigated the advantages of FOPID controllers in terms of performance, robustness, stability and accuracy in industrial heating and temperature control systems. Using application examples such as temperature control of ambulances and bioreactors, the improvements of FOPID controllers over classical PID controllers are presented in a comprehensive analysis. By combining an inverse solution with a PD controller that does not require readjustment under changing conditions, Haghighi et al.[34] created a control system for two- and three-dimensional temperature control of functionally graded plates. This method was able to manage the temperature of the plates in both dimensions. Pringsakul and Puangdownreong[35] introduced a modified flower pollination algorithm (MoFPA), which is a better version of the original flower pollination algorithm (FPA). The purpose of this MoFPA was to increase the search performance. In order to regulate the temperature of an electric heating furnace, they developed a PIDA control system with the help of the MoFPA project that was offered. In comparison to the PID control system, they discovered that the proposed control system achieved a higher level of efficiency. Wang et al.[36] proposed a fuzzy PID control system optimized with the WOA to overcome the shortcomings of conventional control methods in applications such as perovskite solar cells and reduced the response time and overshoot rate with this system. Alzakari et al.[37] presents an innovative framework by combining the modified electric eel foraging optimization algorithm (mEEFO) with a filtered PID controller (PIDN), which is used for the first time in electric furnace temperature control to achieve better performance even under challenging conditions such as external factors and measurement noise. Gani et al.[1] improve critical performance metrics such as overshoot, settling and rise time with a genetic algorithm (GA)-

based PID controller using the integral of absolute error (IAE), making an important contribution especially for the food and pharmaceutical industries that require fast temperature control. Zhang et al.[38] conducted an experiment in which they applied a technique that was developed for fractional order model predictive control (FMPC) to a temperature model of an industrial heating furnace. The discretization of the suggested technique is accomplished by the utilization of the fractional order Grunwald-Letnikov definition, and the production of control signals is accomplished through the reduction of the cost function. For the purpose of tuning the PID controller, Sinlapakun et al.[39] utilized the Nelder-Mead (NM) approach, with the IAE serving as the desired cost function. They demonstrated that the Ziegler-Nicholes (ZN), Cohen-Coon (CC), and direct synthesis (DS) approaches are not as effective as the technique that they developed.

The chosen controller type for this investigation is RPIDD^2, a variant of PID used for regulating electric furnaces. RPIDD^2 differs from the classic PID controller by the inclusion of an additional second-order derivative component (D^2). This component offers more flexibility and accuracy when controlling more complex structures of dynamic systems. The non-linear and time-varying characteristics of electric furnaces pose a challenge for the classic PID controller. The RPIDD^2 controller improves stability by better adapting to such complex systems. It also offers significant advantages in terms of energy efficiency and accuracy. Several studies in the literature deal with the application of PIDD^2 controllers. One notable study presents an innovative method to optimize the PIDD^2 controller for the automatic voltage regulator (AVR) of synchronous generators. This proposed method not only reduces load disturbances but also improves performance compared to conventional PID controllers. Its effectiveness has been validated by experimental tests under real-world conditions[40]. Another study presents a robust PIDD^2 controller for load frequency control (LFC) in time-delayed power systems, which aims to reduce the performance losses caused by communication time delays (CTDs)[41]. The controller was optimized using the Kharitonov stability theorem and the internal model control (IMC) approach. It showed high robustness and effectiveness in the presence of parameter uncertainties and sudden load disturbances. Li and colleagues[42,43] proposed the tuning of PID and PIDD^2 controllers for time-delayed integration processes using the state-space pole placement method in two separate studies. Their observer-based structure reduces sensitivity to measurement noise while achieving balanced performance in terms of robustness, disturbance rejection and noise attenuation. In another study[44], a state-space-based PIDD^2 (SS-PIDD^2) control method was proposed to consider the effects of time delays in wind turbine pitch control. The simulation results showed that SS-PIDD^2 outperformed classical methods by balancing robustness, performance and reducing measurement noise. This study is the first to address the application of the real PIDD^2 (RPIDD^2) controller in temperature control, particularly in the context of electric furnace operation. The existing literature points out the gap in this area and the proposed method is expected to make an important contribution to address this shortcoming. While the literature highlights significant advances in the application of PIDD^2 controllers, effective implementation often depends on the optimization techniques used. Given the inherent complexity of dynamic systems such as electric furnaces, the selection of a robust optimization algorithm is critical to unlock the full potential of the RPIDD^2 controller. Achieving this requires innovative approaches that push the limitations of existing optimization methods.

Metaheuristic algorithms are characterized by their advantages, such as the fact that they do not require all system equations and are only minimally influenced by the system complexity (e.g. simple/complex structures or the number of variables to be optimized)[45–47]. However, despite their effectiveness for certain types of problems, existing algorithms are often inadequate as they struggle with limitations such as premature convergence and slow convergence speed. Rapidly evolving industries produce challenging optimization problems that may not be effectively solved with current techniques[48]. This necessitates the development of new algorithms and the improvement of existing methods to enhance their efficiency in overcoming a variety of technical challenges. To overcome these shortcomings, a new optimization method, quadratic interpolation optimization (QIO) algorithm, is proposed in this paper for temperature control in electric furnaces. The QIO[49] utilized in this study aims to tune the RPIDD^2 controller for temperature control in electric furnaces, thus improving the efficiency of the system through precise and adaptive parameter adjustments to the complex structure of control systems. QIO is a new mathematically based optimization approach. This algorithm can successfully overcome the limitations of traditional second-order interpolation. The best solution for the least value of an area formed by any three points can be found by it in a quick and precise manner to find the ideal answer. In particular, the optimal solution of the optimization object can be obtained in a number of iterations with a minimum amount of computational effort and a high degree of precision. In addition, this is an excellent method for solving models with a high level of complexity and situations in which the target object has unknown expressions. These properties make QIO a suitable alternative for achieving temperature targets with high accuracy in complex systems such as electric furnaces.

We perform a comprehensive evaluation of the proposed control method (QIO-RPIDD^2) using various statistical performance analyses, the Wilcoxon signed-rank test, time and frequency response analyses, and convergence analyses. In addition, a comparative analysis of the proposed approach with metaheuristic algorithms such as the flood optimization algorithm (FLA)[50], the reptile search optimization algorithm (RSA)[51], particle swarm optimization (PSO)[52] and differential evolution (DE)[53] is performed. FLA and RSA are compared because they are the most up-to-date and effective algorithms. We chose PSO and DE because these are the most commonly used algorithms in the literature. The population size, the number of iterations and other specific hyperparameters for the algorithms were set according to the values proposed in the relevant literature[50–53]. The obtained results show that the proposed new QIO-RPIDD^2 control method can significantly improve the performance of the temperature control system and the overall efficiency of the system compared to these techniques.

Quadratic interpolation optimization algorithm

The quadratic interpolation method is a widely used approach to curve fitting and is usually applied to individual functions to determine the minimum point in a given output interval. A quadratic interpolation polynomial $L(x)$ is used to estimate the function $f(x)$ and determine its minimum point. Determining the minimizer of the polynomial $L(x)$ gives the estimated minimum point of the function $f(x)$[49]. The primary formulation of quadratic interpolation is as follows:

$$L(x) = \alpha^{2} + \beta x + \delta\,;\ \alpha, \beta, \delta \in R \tag{1}$$

Here α, β, γ are uncertain coefficients. In this case, assume that $f(x)$ has three points.

$$P_i = (x_i, f(x_i))\,;\ P_j = (x_j, f(x_j))\,;\ P_k = (x_k, f(x_k)) \tag{2}$$

And for the interpolation conditions $a \leq x_i < x_j < x_k \leq b$, $f(x)$ is equal to $L(x)$ at the interpolation points. In this case, x_i, x_j ve x_k are expressed as follows.

$$L(x_i) = \alpha {x_i}^2 + \beta x_i + \delta = f(x_i)\,;\ L(x_j) = \alpha {x_j}^2 + \beta x_j + \delta = f(x_j)\,;\ L(x_k) = \alpha {x_k}^2 + \beta x_k + \delta = f(x_k) \tag{3}$$

To find the minimum of $L(x)$, the derivative of Eq. (1) is taken and set to 0 (zero). The minimizer x^* is expressed as in Eq. (4):

$$x^* = -\frac{\beta}{2\alpha} \tag{4}$$

Then α and β are found by solving Eqs. (5) and (6).

$$\alpha = \frac{(x_j - x_k) f(x_i) + (x_k - x_i) f(x_j) + (x_i - x_j) f(x_k)}{(x_j - x_k)(x_k - x_i)(x_i - x_j)} \tag{5}$$

$$\beta = -\frac{\left(x_j^2 - x_k^2\right) f(x_i) + \left(x_k^2 - x_i^2\right) f(x_j) + (x_i^2 - x_j^2) f(x_k)}{(x_j - x_k)(x_k - x_i)(x_i - x_j)} \tag{6}$$

In this case, the substitution of α and β in Eqs. (5) and (6) in Eq. (4) yields Eq. (7):

$$x^* = -\frac{\left(x_j^2 - x_k^2\right) f(x_i) + \left(x_k^2 - x_i^2\right) f(x_j) + (x_i^2 - x_j^2) f(x_k)}{2 \cdot [(x_j - x_k) f(x_i) + (x_k - x_i) f(x_j) + (x_i - x_j) f(x_k)]} \tag{7}$$

After all these steps, you can obtain the second-order interpolation polynomial $L(x)$ as follows:

$$L(x) = \frac{(x - x_j)(x - x_k)}{(x_i - x_j)(x_i - x_k)} f(x_i) + \frac{(x - x_i)(x - x_k)}{(x_j - x_i)(x_j - x_k)} f(x_j) + \frac{(x - x_i)(x - x_j)}{(x_k - x_i)(x_k - x_j)} f(x_k) \tag{8}$$

The exploration phase of the QIO algorithm aims to discover new regions in the search space. This helps the algorithm to avoid premature convergence and to avoid getting stuck in local minima. This process is performed in three steps: Point selection x_i, x_j, x_k, cubadic interpolation (x_j^*, the best predicted point for the solution) and position update. The mathematical expression for the update in the exploration phase is as in Eq. (9) and Eq. (10):

$$v_i(t+1) = x^*_{i,rand1,rand2}(t) + w_1 * \left(x_{rand3}(t) - x^*_{i,rand1,rand2}(t)\right) + round(0.5 * (0.05 + r_1)) * log\frac{r_2}{r_3} \tag{9}$$

$$x^*_{i,rand1,rand2}(t) = GQI(x_i(t), x_{rand1}(t), x_{rand2}(t), f(x_i(t)), f(x_{rand1}(t)), f(x_{rand2}(t)) \tag{10}$$

Here $x^*_{i,rand1,rand2}(t)$ is the minimizer determined using the generalized quadratic interpolation (GQI) method for the current individual and two randomly selected individuals. w_1, r_1, r_2 and r_3 are control parameters that set the balance between search (exploration) and deeper inspection (exploitation).

In the exploitation phase of the QIO algorithm, the algorithm focuses on improving the best available solutions. The updated position in the exploitation phase is calculated as in Eq. (11) and Eq. (12):

$$v_i(t+1) = x^*_{best,rand1,rand2}(t) + w_2 \cdot \left(x_{best}(t) - round(1 + rand)\right) \cdot \left(\frac{Ub - Lb}{Ub^{rD} - Lb^{rD}}\right) \cdot x_i^{rD} \tag{11}$$

$$x^*_{best,rand1,rand2}(t) = GQI(x_{best}(t), x_{rand1}(t), x_{rand2}(t), f(x_{best}(t)), f(x_{rand1}(t)), f(x_{rand2}(t)) \tag{12}$$

Once the exploration and exploitation has been performed, the position of each individual is updated according to the calculated minimizers. In this context, the following Eq. (13) is used.

$$x_i(t+1) = \begin{cases} x_i(t)\,; f(x_i(t)) \leq f(v_i(t+1)) \\ v_i(t+1)\,; f(x_i(t)) > f(v_i(t+1)) \end{cases} \tag{13}$$

The QIO algorithm's flowchart is depicted in (Fig. 1). As demonstrated it begins by defining its control parameters, which include population size, maximum iterations, and other relevant variables necessary for its operation. Following this, an initial population of potential solutions is generated, and the fitness values of these individuals are calculated to assess their quality with respect to the optimization objective. The algorithm then checks whether the stopping criteria (reaching the maximum number of iterations), have been met. If not, two individuals are randomly selected from the population for further processing. Based on a probabilistic decision threshold ($rand > 0.5$), the algorithm either applies exploration or exploitation mechanisms. For exploration ($rand \leq 0.5$), the minimizer of the GQI function is determined using the current individual and two randomly selected individuals, followed by applying an exploration update using Eq. (9). For exploitation $(rand > 0.5)$, the minimizer of the GQI function is calculated using the best solution found so far along with two randomly selected individuals, and the exploitation update is performed using Eq. (11). Subsequently, the i^{th} individual is updated using Eq. (13) based on the outcome of the chosen mechanism. Throughout the process, the algorithm maintains a record of the best solution identified so far. The procedure iterates until the stopping condition is satisfied, at which point the algorithm outputs the optimal solution and terminates. This iterative framework ensures a balanced trade-off between exploration of new solution spaces and exploitation of the best solutions, thereby enhancing the algorithm's ability to solve complex optimization problems effectively.

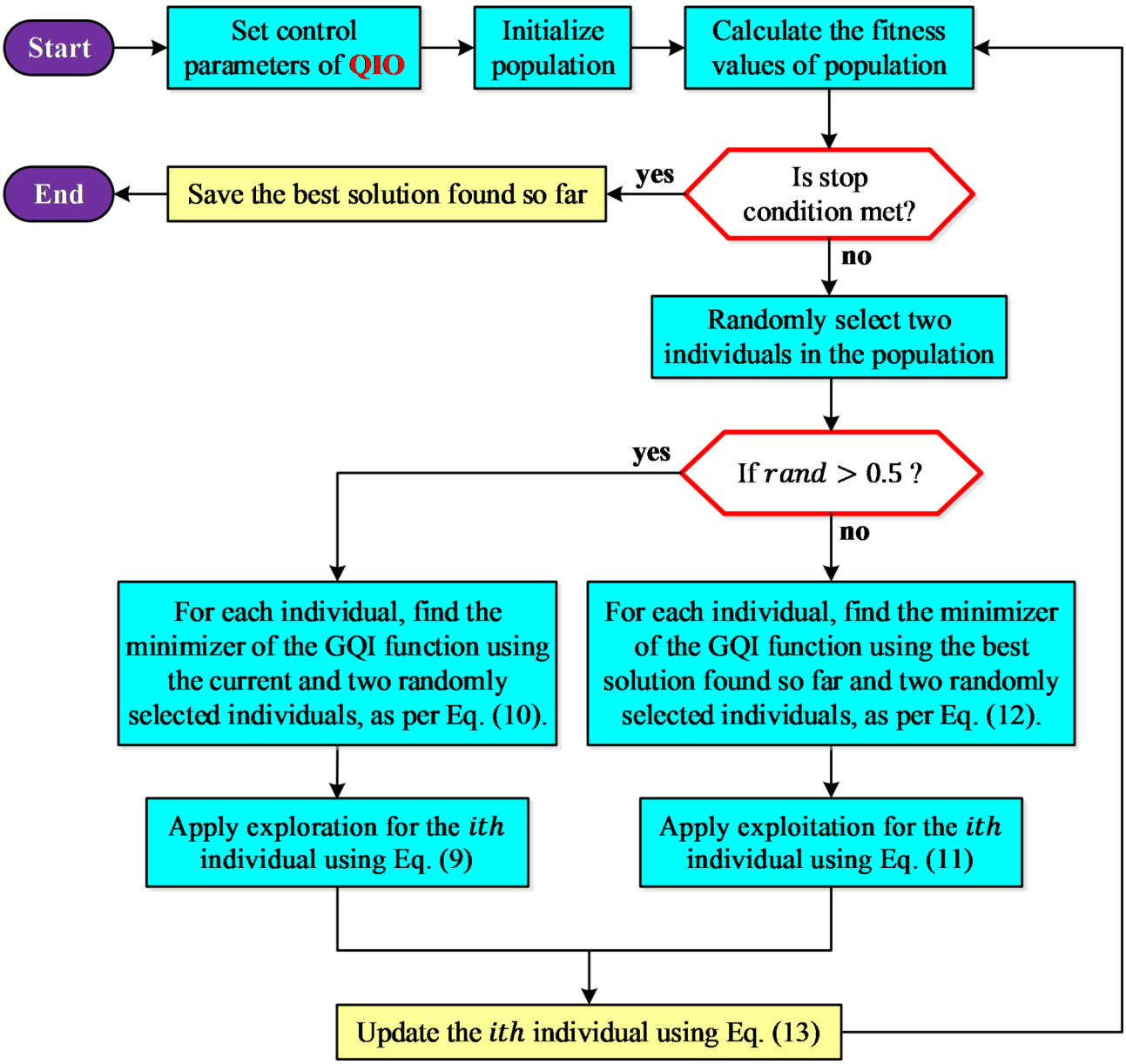


Fig. 1. Essential steps of QIO.

Modeling of electric furnace temperature control system

In electric furnaces, temperature control is a dynamic system and control algorithms are used to maintain the temperature at the desired value. In this system, the temperature is set to an appropriate level and deviations are minimized by control mechanisms. The temperature control system normally evaluates the internal temperature in the furnaces using sensors and modulates the heating components via various controllers.

The reference signal in the temperature control system in Fig. 2 is the target temperature value that the system should reach. The measured temperature value is the actual temperature of the system at that time. The error signal is the difference between the reference temperature and the measured temperature. This difference is corrected by the controller. The mathematical model is expressed as follows:[37]

$$G(s) = \frac{b_0}{a_2 s^2 + a_1 s + a_0} e^{-Ds} \tag{14}$$

The first-order Padé approach is used in temperature control to simulate the delayed response of industrial furnaces or process control systems. With this method, time-delayed systems can be controlled more reliably and precisely. First-order Padé approximation:

$$e^{-Ds} \cong \frac{2 - Ds}{2 + Ds} \tag{15}$$

If the time delay is also replaced, the transfer function of the system is expressed as follows:

$$G(s) = \frac{b_0(2 - Ds)}{(a_2 s^2 + a_1 s + a_0)(2 + Ds)} \tag{16}$$

In this statement, b_0 is the gain coefficient of the system, $a_2 s^2 + a_1 s + a_0$, is the denominator polynomial that determines the dynamic behavior of the system and D is the parameter for the time delay of the system. The transfer function expressed in the first-order Padé approximation helps to model the dynamics of systems with delayed response, such as electric furnaces, more accurately. This function creates a realistic simulation of the system by considering the effect of the delay in the input-output relationship of the system. In particular, the term $\frac{(2-Ds)}{(2+Ds)}$, which represents the delay, changes the gain of the system depending on the frequency and the delay time.

Structure of real PID plus second-order derivative (RPIDD2) controller for temperature control system

The RPIDD^2 controller provides more advanced control by adding a second derivative term to the conventional PID controller. This reduces overshoot, rise, settling times, resulting in better performance in temperature control systems, especially those with fast dynamics. The reason for using the RPIDD^2 controller is its ability to improve phase margin, steady state accuracy and stability. The following equation is used to describe the RPIDD^2 controller[6,7].

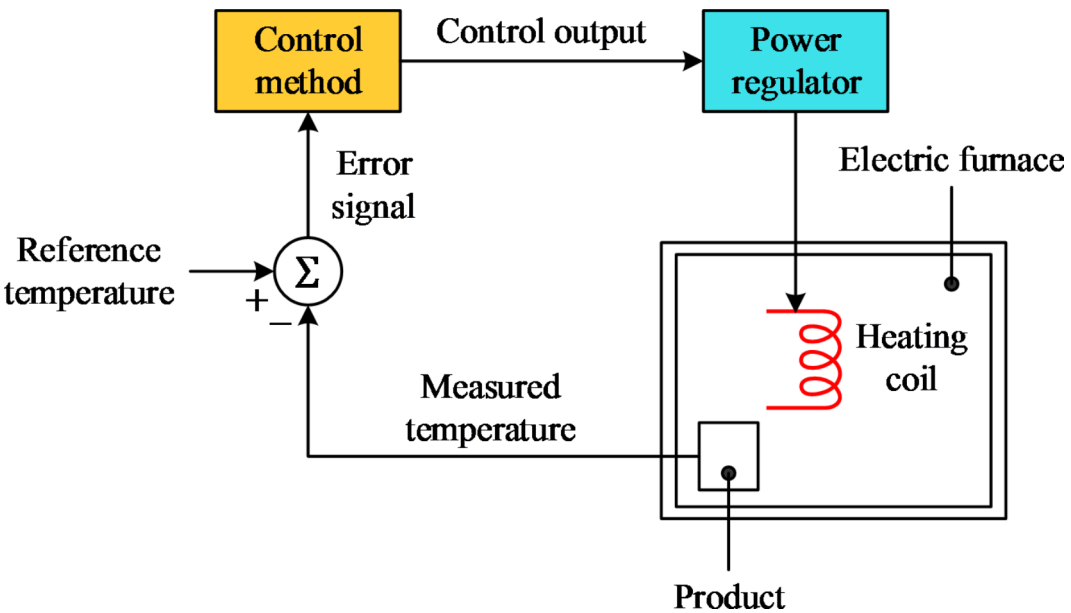


Fig. 2. Block diagram of temperature control system.

$$C(s) = K_p + \frac{K_i}{s} + K_{d1}\frac{N_1 s}{s+N_1} + K_{d2}\left(\frac{N_2 s}{s+N_2}\right)^2 \tag{17}$$

where K_p, K_i, K_{d1} and K_{d2} are respectively proportional, integral, derivative and double derivative gains respectively. In addition, N_1 and N_2 stand for the filter coefficients. The block diagram in Fig. 3 shows the general structure of the RPIDD^2 controller. The RPIDD^2 controller ensures both a fast response and steady state by providing a versatile response to error signals in the system. The two derivative gains are particularly effective here for precise control and fast system response. The main advantage of the RPIDD^2 controller is that it can provide smoother and faster responses for higher order systems within acceptable limits for overshoot and settling time[6].

The closed loop transfer function describes the interaction between the input and the output of the system, including the action of the controller, and is expressed as follows.

$$T_{closed-loop}(s) = \frac{C(s)G(s)}{1 + C(s)G(s)} \tag{18}$$

In here, $C(s)$ is the controller and $G(s)$ is the open-loop transfer function of the system. The closed-loop transfer function plays an important role in analyzing the behavior of the system in a feedback loop, as it determines the accuracy of the system in reaching the target, the settling time and the overall stability. This transfer function aims to operate the system more accurately and reliably by taking into account the effects of the controller parameters on the system dynamics. If, for example, varying the gain and damping ratios in the system, this has a direct effect on the response of the closed control loop. A properly tuned $C(s)$ controller can provide advantages such as shorter stabilization time, lower steady-state error and less susceptibility to external influences in the closed-loop system, which can improve the efficiency and stability of the system.

A novel approach: QIO-based RPIDD2 controller design

The proposed approach was developed for temperature control systems in electric furnaces to improve the performance of systems that respond to rapid changes. This approach, which is a combination of the QIO algorithm and the RPIDD^2 controller, improves the effectiveness of the system by making precise and adaptive parameter settings for the complex structures of the control systems. The following parameters were used in this study. These parameters are common parameters used in studies dealing with different optimization and control approaches in electric furnace temperature control. In our study, $a_0 = 0.2$, $a_1 = 1.1$, $a_2 = 1$, $b_0 = 0.15$ and the delay time $D = 1.5$ were set as common parameters to ensure consistency with the results in all other studies[1,37,39].

$$G(s) = \frac{-0.1125s + 0.15}{0.75s^3 + 1.825s^2 + 1.25s + 0.2} \tag{19}$$

Zwe-lee gaing (ZLG) objective function was used to minimize the performance criteria of dynamic response such as maximum overshoot, steady-state error, settling time and rise time[54].

$$ZLG = \left(1 - e^{-\theta}\right)\left(\frac{O_{shoot} + S_{error}}{100}\right) + e^{-\theta}\left(t_{set} - t_{rise}\right) \tag{20}$$

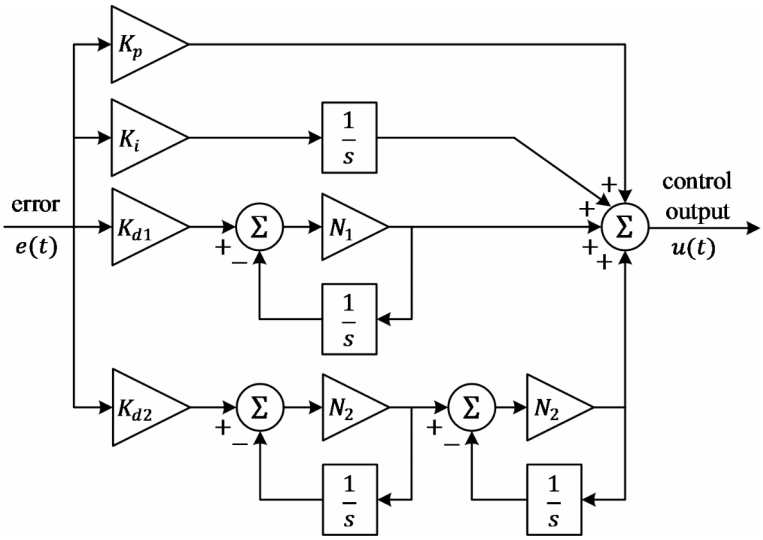


Fig. 3. Block diagram of RPIDD^2 controller.

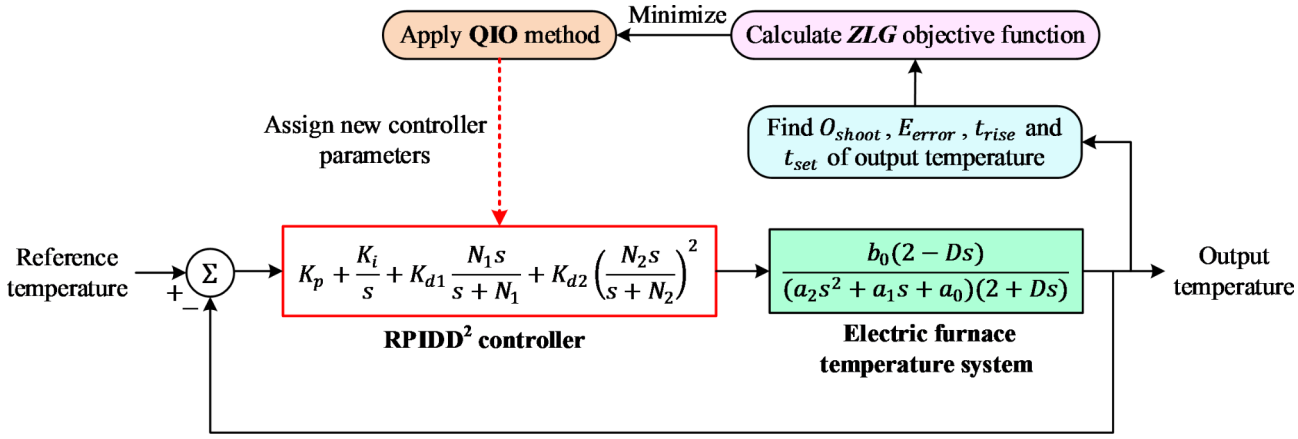


Fig. 4. Block diagram of novel QIO-based RPIDD² controlled system.

Algorithms	Parameter settings
QIO	–
FLA	$Ne = 5$
RSA	$\alpha = 0.1,\ \beta = 0.1$
PSO	$w = 0.6,\ c_1 = 2,\ c_2 = 2$
DE	$Scaling\ factor = 0.5,\ \ crossover\ probability = 0.5$

Table 1. Parameter settings of algorithms.

In order to find the best solution within the limits given below, it is necessary to adjust the control parameters (K_p, K_i, K_{d1}, K_{d2}, N_1, and N_2) using the proposed approach, the QIO method. The aim is to minimize the performance criteria such as percentage overshoot (O_{shoot}), percent steady state error (S_{error}), settling time (t_{set}) and rise time (t_{rise}) for the temperature control of the electric furnace. A cost function is defined according to these performance criteria with a weighting factor $(\theta = 1)$. The constraints given in Eq. (21) were considered.

$$0.1 \le K_p \le 10;\ 0.1 \le K_i \le 1;\ 0.1 \le K_{d1} \le 10;\ 0.1 \le K_{d2} \le 1;\ 10 \le N_1 \le 500;\ 10 \le N_2 \le 500 \quad (21)$$

The best solution resulting from optimization is the set of parameters that optimize system performance within certain limits. These settings provide criteria such as minimum overshoot, low steady state error, short settling time and fast rise time. The block diagram in Fig. 4 shows the model of the temperature control system of the electric furnace.

Within this model, the QIO method and the RPIDD² controller are the main components of this structure. QIO minimizes the error, overshoot, rise time and settling time of the system by adjusting the gains of the RPIDD² controller. The process runs in a feedback loop to minimize the difference between the reference temperature and the furnace output temperature. In this way, the RPIDD² controller optimized by the QIO method ensures faster, more accurate and more stable performance of the electric furnace temperature control system. Section 6 describes the results of the proposed controlled system and its comparison with different control methods.

Simulation results

Compared metaheuristic algorithms

In order to provide a comprehensive and robust analysis in evaluating the proposed QIO-RPIDD² control method, the FLA, RSA, PSO and DE algorithms are selected for comparison. The selection of these algorithms is based on the criteria of timeliness and efficiency as well as widespread use and validation in the literature. FLA and RSA are the most recent developments in the field of meta-heuristic algorithms and have shown high performance on complex optimization problems. These algorithms are suitable candidates for evaluating a new algorithm such as QIO in a comparative study by optimizing them with parameters such as the number of environmental agents ($Ne = 5$) and the exploration-exploitation ratio ($\alpha = 0.1$), ($\beta = 0.1$). PSO and DE are among the most widely used meta-heuristic algorithms in the literature due to their simplicity, robustness and efficiency in various optimization problems and have been implemented with parameters such as inertia weight ($w = 0.6$), cognitive ($c_1 = 2$) and social coefficients ($c_2 = 2$), scaling factor (0.5) and crossover probability (0.5). The inclusion of these algorithms provides a solid basis for comparing the performance of QIO with current and widely used methods in the literature.

Table 1 shows that QIO does not require any parameter settings other than the population size and the number of iterations. This simplifies the optimization process, and the algorithm can be adapted quickly. This

Index	QIO	FLA	RSA	PSO	DE
Best	**0.5612**	0.5990	0.6299	0.6482	0.6672
Worst	**0.6413**	0.6886	0.7675	0.7587	0.7527
Median	**0.5866**	0.6258	0.6493	0.6673	0.6921
Mean	**0.5916**	0.6291	0.6591	0.6762	0.6963
Standard deviation	**0.0215**	0.0246	0.0320	0.0256	0.0241

Table 2. Statistical metrics of *ZLG* optimized by various algorithms.

QIO versus FLA		QIO versus RSA		QIO versus PSO		QIO versus DE	
p-value	Superior	p-value	Superior	p-value	Superior	p-value	Superior
9.0421E−05	QIO	1.2290E−05	QIO	1.2290E−05	QIO	1.2279E−05	QIO

Table 3. Wilcoxon signed-rank test results.

simple structure makes QIO superior to other algorithms in terms of ease of implementation and can also be used effectively in applications that require high precision, such as temperature control.

Statistical analysis

Table 2 shows the results of the statistical analysis of the algorithms. All algorithms were tested with 25 runs each. The population size was set to 30 and the maximum number of iterations to 100. These parameters were kept constant to compare the performance of the individual algorithms.

QIO seems to have the best performance in all metrics. The fact that it has the lowest best, worst, median and mean values shows that it achieves the most optimal results when minimizing the ZLG objective function. FLA provides the second-best results, followed by the QIO algorithm. RSA has the highest worst value and the highest standard deviation, indicating that its performance results are more variable. This shows the inconsistency of the results. PSO and DE show strong performances but give worse results than QIO. The higher mean and worst values indicate that these algorithms are not as consistent as QIO. The standard deviation values show that RSA is the most variable, DE provides more stable results, but QIO is by far more consistent than the others.

Wilcoxon signed-rank test

The Wilcoxon signed-rank test is frequently used, especially in performance comparisons of optimization algorithms. It is suitable for testing whether the results of one algorithm differ statistically significantly from the results of another algorithm. If the p-value is smaller than the specified significance level (usually 0.05), it is concluded that there is a significant difference between the two groups[6]. Table 3 shows the results of the Wilcoxon signed-rank test. These results show that the QIO algorithm statistically outperforms the other algorithms. The p-values for each comparison are well below the significance level of 0.05, indicating that QIO is clearly superior to the other algorithms.

Convergence curve of objective function

Figure 5 compares the performance of the QIO algorithm in minimizing the ZLG objective function with other algorithms. This figure shows the convergence rates and the values of the ZLG objective function as a function of the number of iterations. Table 4 contains the numerical values of the RPIDD² controller parameters optimized using QIO and other algorithms.

When the optimal RPIDD² parameter values in Table 4 are substituted into the overall transfer function, they are obtained separately for each algorithm as follows. The closed loop transfer functions show the effects of the RPIDD² controllers optimized with the QIO, FLA, RSA, PSO and DE algorithms on the electric furnace temperature control system. Each transfer function expresses numerically how the parameter selection of the algorithm influences the system dynamics.

$$TF_{QIO}(s) = \frac{-640.4s^5 - 1.781e05s^4 - 7.42e05s^3 + 6.397e05s^2 + 7.697e05s + 1.609e05}{0.75s^7 + 376.2s^6 + 3.839e04s^5 + 1.018e06s^4 + 2.005e06s^3 + 2.488e06s^2 + 1.064e06s + 1.609e05} \quad (22)$$

$$TF_{FLA}(s) = \frac{-1836s^5 - 5.134e05s^4 - 2.039e06s^3 + 1.755e06s^2 + 2.158e06s + 4.672e05}{0.75s^7 + 398.5s^6 + 6.244e04s^5 + 2.823e06s^4 + 5.808e06s^3 + 7.074e06s^2 + 3.006e06s + 4.672e05} \quad (23)$$

$$TF_{RSA}(s) = \frac{-1.969e04s^5 - 4.506e06s^4 - 1.753e07s^3 + 1.227e07s^2 + 2.253e07s + 4.019e06}{0.75s^7 + 839s^6 + 2.819e05s^5 + 2.982e07s^4 + 6.472e07s^3 + 6.834e07s^2 + 3.149e07s + 4.019e06} \quad (24)$$

$$TF_{PSO}(s) = \frac{-286.8s^5 - 5.817e04s^4 - 5.717e05s^3 + 3.935e05s^2 + 5.432e05s + 1.165e05}{0.75s^7 + 331.8s^6 + 3.261e04s^5 + 9.209e05s^4 + 1.673e06s^3 + 1.903e06s^2 + 7.833e05s + 1.165e05} \quad (25)$$

$$TF_{DE}(s) = \frac{-244.5s^5 - 8820s^4 - 2.633e04s^3 + 1.987e04s^2 + 3.706e04s + 6578}{0.75s^7 + 98.91s^6 + 4126s^5 + 5.907e04s^4 + 1.209e05s^3 + 1.171e05s^2 + 5.244e04s + 6578} \quad (26)$$

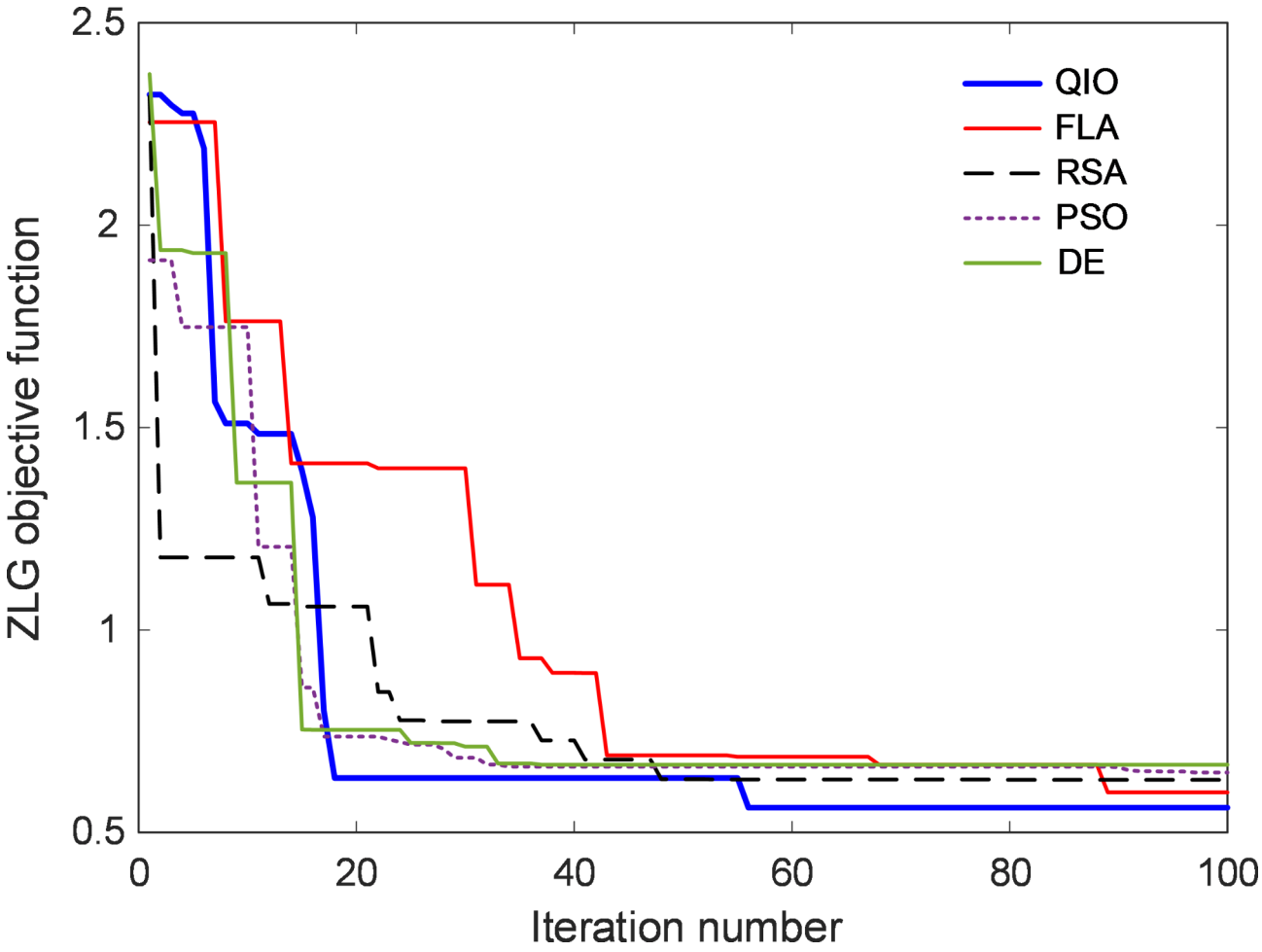


Fig. 5. Change of ZLG objective function.

Control methods	K_p	K_i	K_{d1}	K_{d2}	N_1	N_2
QIO-RPIDD^2	4.0117	0.7295	5.7891	0.8959	373.7615	62.7211
FLA-RPIDD^2	3.9277	0.7342	5.6363	0.9881	284.8655	122.0280
RSA-RPIDD^2	3.7970	0.5981	4.6436	0.8784	226.1581	445.0483
PSO-RPIDD^2	3.4782	0.6468	4.6869	0.2800	316.7752	61.5627
DE-RPIDD^2	3.5998	0.5703	4.1947	0.8769	33.2147	48.1141

Table 4. Best RPIDD^2 parameters found by various algorithms.

Time response analysis

Figures 6 and 7; Table 5 compare the time response and performance metrics of RPIDD^2 controllers optimized with different algorithms in a temperature control system for an electric furnace. Figure 6 shows the overall time response of the system, while Fig. 7 shows a detailed view of this behavior so that we can better observe the small differences in the performance of each algorithm. Table 5 numerically summarizes the performance metrics such as rise time (t_{rise}), settling time (t_{set}), percent overshoot (O_{shoot}), and percent steady state error (S_{error}). According to Table 5, QIO-RPIDD^2 has the shortest rise and settling time and the lowest overshoot and error in the steady state. These results allow the interpretation that the QIO algorithm provides the fastest and most stable response and outperforms the other algorithms in temperature control. The FLA-RPIDD^2 and PSO-RPIDD^2 algorithms perform similarly well to QIO, but lag behind QIO in terms of overshoot and settling time. DE-RPIDD^2 has the longest rise and settling time and the highest steady-state error, indicating that DE is slower and less precise in temperature control compared to the other algorithms.

Frequency response analysis

The graph in Fig. 8 shows the frequency response of RPIDD^2 controlled open loop systems optimized with the algorithms QIO, FLA, RSA, PSO and DE in Bode diagram format. The upper part shows the gain

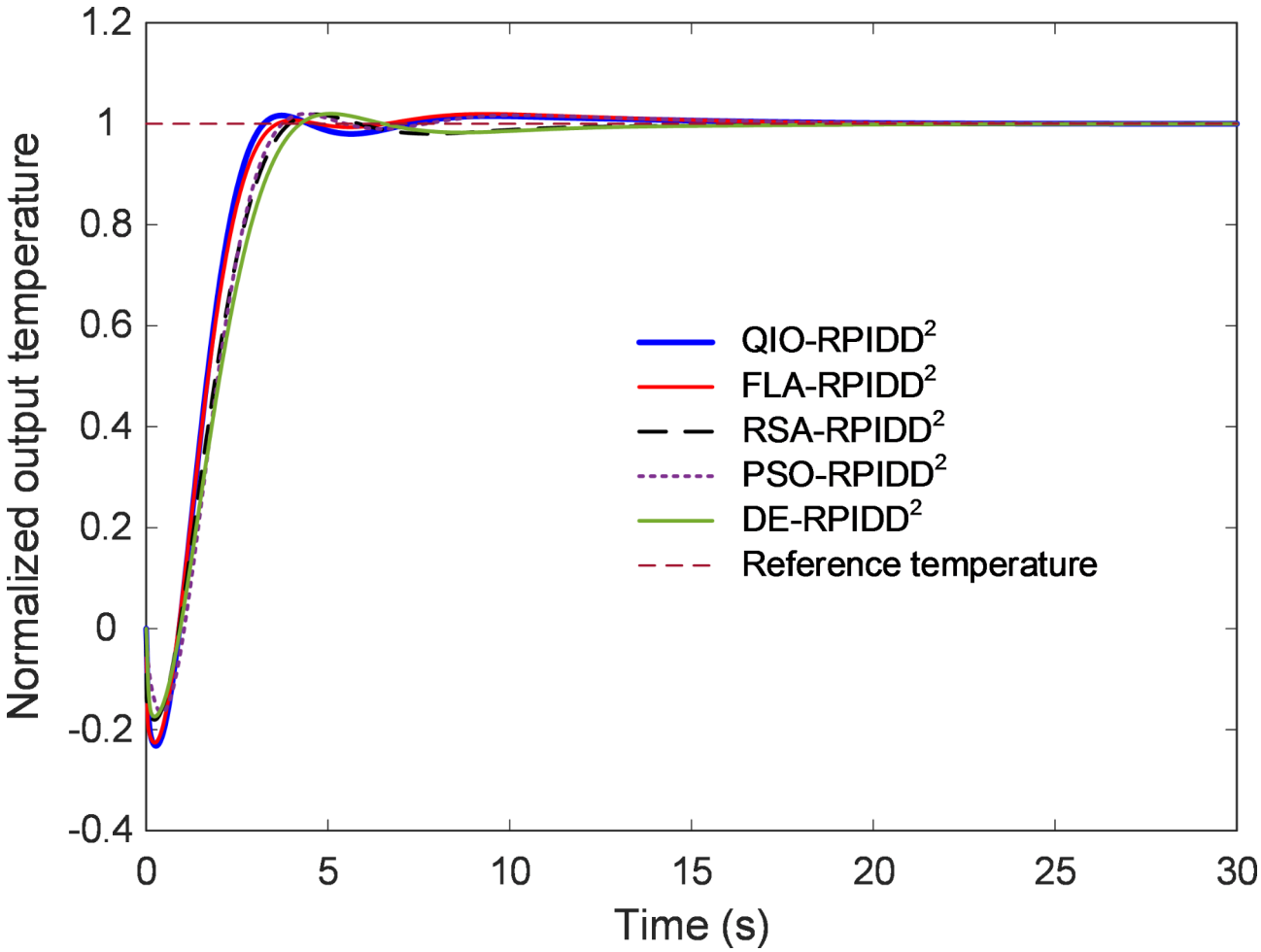


Fig. 6. Comparative analysis of closed-loop step responses for electric furnace temperature control system.

curve (amplitude) and the lower part the phase curve. The frequency response analysis is an important tool for evaluating the stability of the system. Phase margin P_{margin} and gain margin G_{margin} are important parameters that determine whether the system is stable or not, while bandwidth B_{width} is an important parameter that determines how quickly the system responds to transients. Table 6 shows the parameter values obtained from this diagram.

G_{margin}, indicates the maximum amount by which the gain of the system can be increased and how much increase the system can tolerate before it becomes unstable. P_{margin}, indicates how much the phase angle of the system can be changed before it becomes unstable. For electric furnaces, the ideal value for P_{margin} is between 30° and 60°. QIO-RPIDD^2 and other algorithms have values around 60°. B_{width}, specifies the maximum frequency range in which the system can operate effectively in a closed control loop. This range allows the system to respond quickly to temperature adjustments while preventing unnecessary frequency components (such as noise) from negatively impacting system performance. Again, according to the results in Table 6, a high QIO-RPIDD^2 bandwidth value is a good criterion and our proposed method has the highest value.

Comparison with documented works

The proposed QIO-RPIDD^2 control method is compared with control methods such as the electric eel foraging optimizer (EEFO)-PIDN[37], the whale optimization algorithm (WOA)-PIDN[37], GA-PID[1] and NM-PID[39]. Figure 9 shows the comparison of the proposed QIO-RPIDD^2 control method with the other control methods EEFO-PIDN, WOA-PIDN, GA-PID and NM-PID in terms of the step response in the closed loop. Figure 9 shows how each control method responds to the step input to the temperature control system. The comparison is based on transient performance metrics such as settling time, overshoot, rise time and steady state error.

Figure 10 is an enlarged view of Fig. 9 and allows us to better recognize the detailed differences in the step response of the closed-loop of the individual control methods. This magnification enables us in particular to investigate the small fluctuations in the transient behavior of the system, the extent of overshoot and the convergence of the individual control methods to the reference temperature. Table 7 shows the comparison between QIO-RPIDD^2 and the other control methods shown in Fig. 10 (EEFO-PIDN, WOA-PIDN, GA-PID and NM-PID) in terms of transient response characteristics.

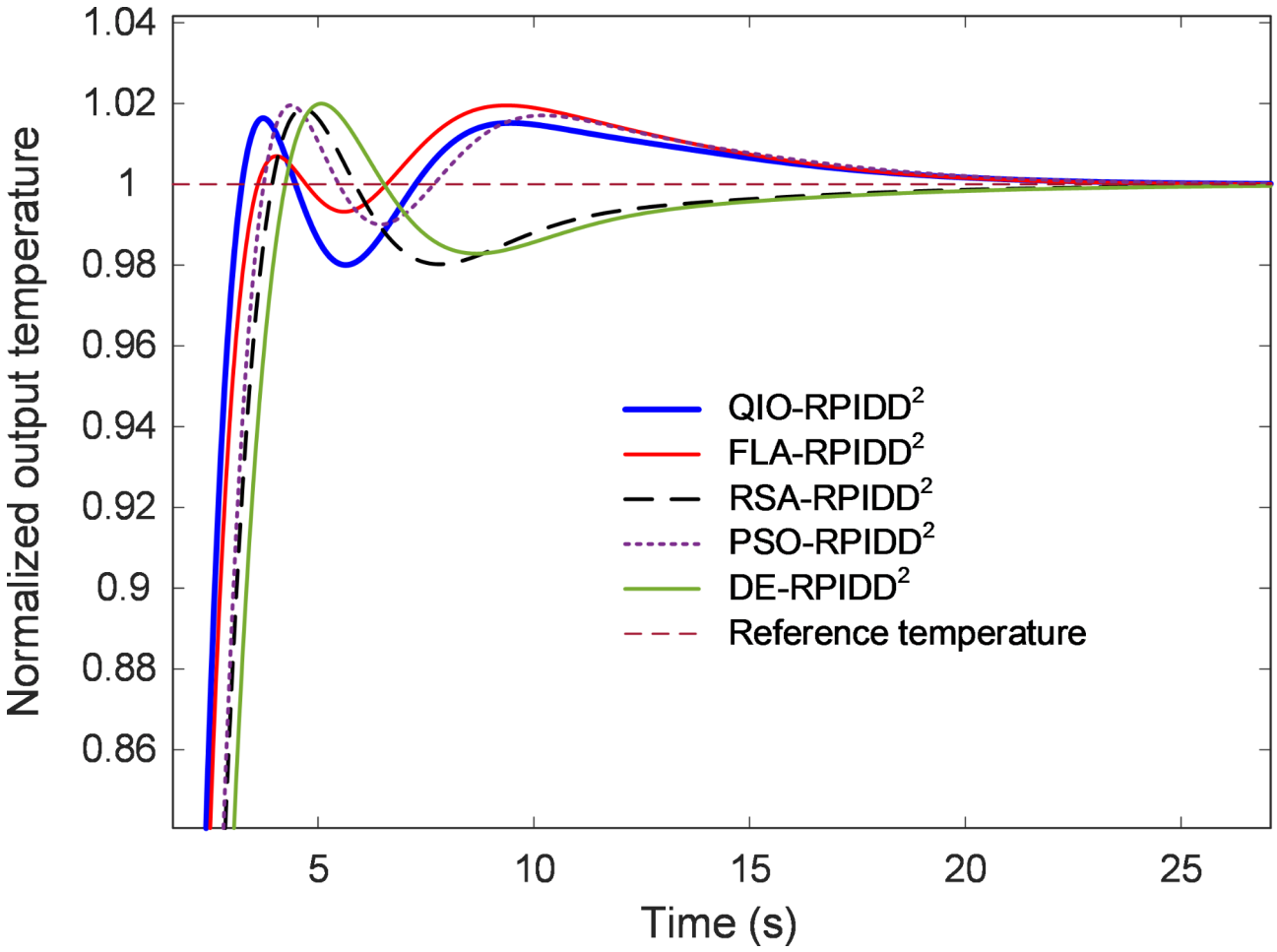


Fig. 7. Enlarged view of (Fig. 6).

Control methods	t_{rise} (s)	t_{set} (s)	O_{shoot} (%)	S_{error} (%)
QIO-RPIDD²	1.5367	3.0340	1.6355	4.5186E − 12
FLA-RPIDD²	1.6795	3.2743	1.9522	6.0174E − 12
RSA-RPIDD²	1.9968	3.6768	1.8687	1.7293E − 08
PSO-RPIDD²	1.7933	3.5218	1.9579	5.7732E − 12
DE-RPIDD²	2.1784	3.9578	1.9959	2.8796E − 08

Table 5. Comparison of transient response specifications.

A detailed analysis of Table 7 shows that our proposed approach QIO-RPIDD² has a fast transient response compared to the other methods with a rise time of 1.5367 s. EEFO-PIDN and WOA-PIDN have longer rise times, which were calculated to be 2.0330 and 1.8674 s, respectively. This means that the system starts slower to reach the target temperature. Although GA-PID and NM-PID have shorter rise times, these methods have more overshoots and fluctuations, making it more difficult to reach a steady state. QIO-RPIDD² has the shortest settling time of 3.0340 s, which means that the system quickly converges to the reference temperature value. EEFO-PIDN and WOA-PIDN have settling times of 4.0212 and 5.4821 s respectively and are therefore longer than QIO-RPIDD². GA-PID and NM-PID, on the other hand, have settling times of over 7 s and take the longest time for the system to reach steady state. This long settling time shows that these methods are not sufficient to reach steady-state of the system quickly. QIO-RPIDD² has the lowest overshoot values with 1.6355%. This shows that the system converges to the reference value without deviating too much. EEFO-PIDN performs similarly well to QIO-RPIDD² with 1.8421% overshoot, but still does not achieve as low an overshoot as QIO-RPIDD². WOA-PIDN shows a higher overshoot of 3.8198%, which means that it has difficulties to stabilize after exceeding the reference value. GA-PID and NM-PID show the highest overshoot values of 3.2725 and 7.0026% respectively. Finally, in terms of steady state error, QIO-RPIDD² has the highest accuracy with a very low steady state error of 4.5186E-12. This shows that the system reaches the value closest to the reference temperature.

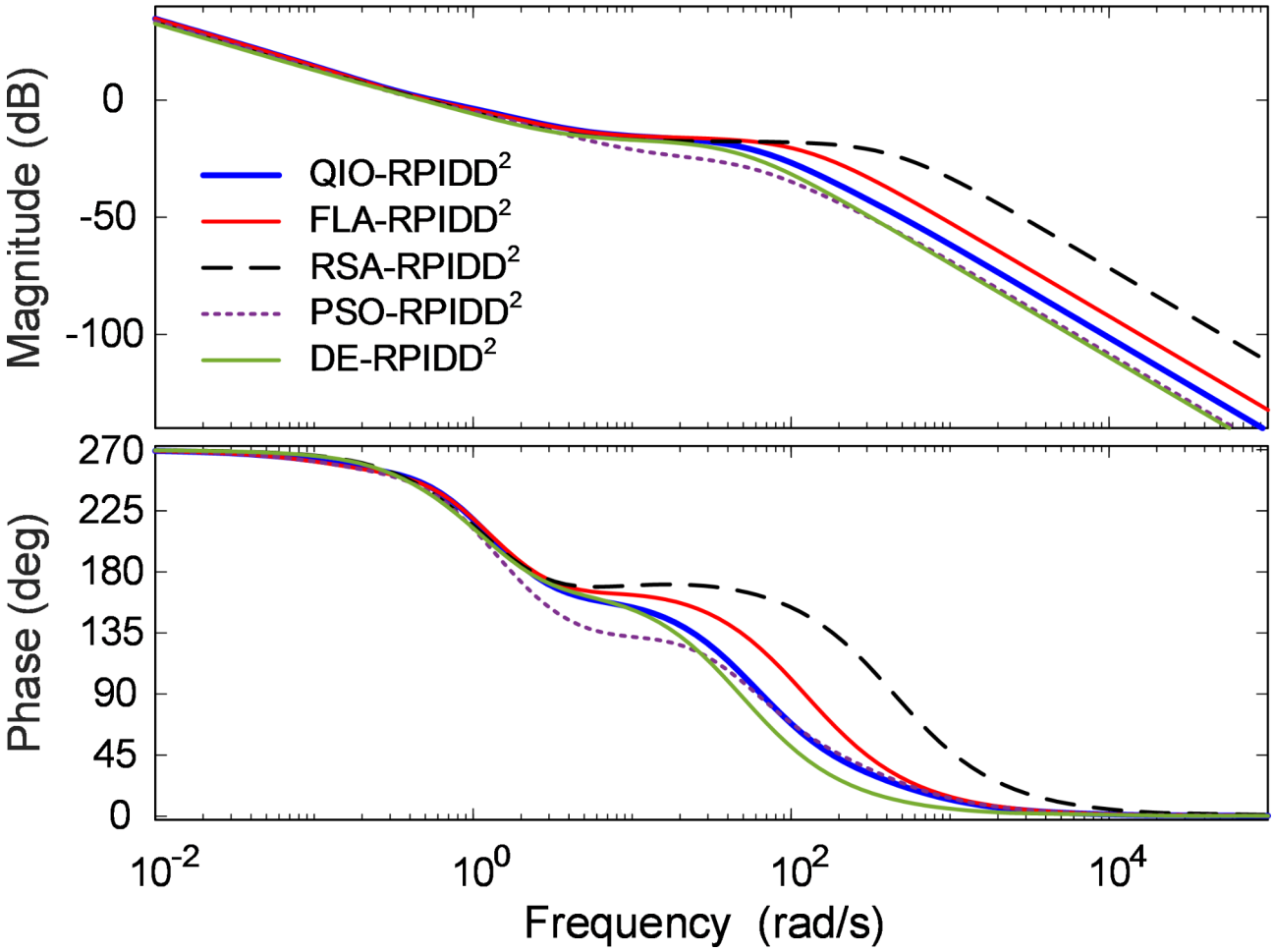


Fig. 8. Bode diagrams of open-loop RPIDD² controlled system.

Control methods	P_{margin} (°)	G_{margin} (dB)	B_{width} (rad/s)
QIO-RPIDD²	61.1612	8.9420	1.8326
FLA-RPIDD²	61.8857	9.7173	1.7149
RSA-RPIDD²	60.4568	11.3069	1.3101
PSO-RPIDD²	61.8342	8.8077	1.4713
DE-RPIDD²	60.7060	11.4770	1.1737

Table 6. Comparison of frequency response specifications.

EEFO-PIDN and WOA-PIDN have a higher steady-state error than QIO-RPIDD² with values of 6.8168E-12 and 3.0287E-11 respectively. GA-PID and NM-PID have the highest steady state error at 1.6148E-07 and 1.0345E-10 respectively.

Figure 11 shows the open-loop Bode plots for the proposed QIO-RPIDD² control method and other control methods (EEFO-PIDN, WOA-PIDN, GA-PID and NM-PID). Table 8 shows that QIO-RPIDD², which has a wide bandwidth with sufficient gain and phase margins, can provide a reliable and effective solution for sensitive temperature control applications such as electric furnaces. Of the other methods, EEFO-PIDN and WOA-PIDN are stable but respond more slowly, while GA-PID and NM-PID are more limited in terms of stability.

Monitoring random reference temperature

Figure 12 shows the temperature response of the proposed QIO-RPIDD² approach to a randomly varying reference temperature. As you can see from the figure, QIO-RPIDD² was able to track the variations of the reference temperature quite coherently. It is noteworthy that the difference between the controlled temperature value and the reference temperature value is very small, especially when the time delay factor is considered. This shows that QIO-RPIDD² has a high performance even under variable conditions and effectively converges to the desired temperature value.

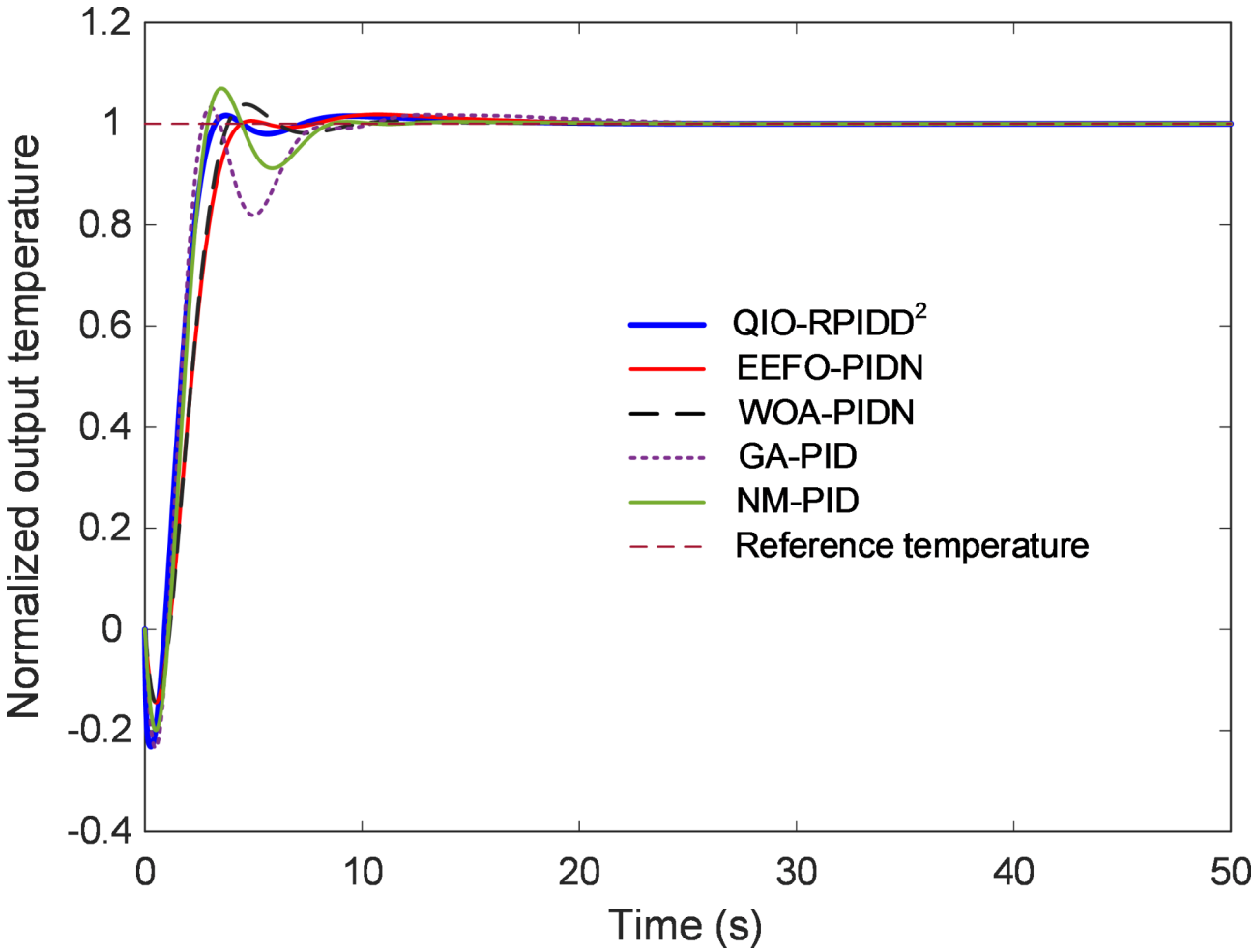


Fig. 9. Comparative analysis of closed-loop step responses for proposed QIO-RPIDD^2 and other reported control methods.

Conclusion and future work

In this study, a novel control approach combining the QIO algorithm with the RPIDD^2 controller was developed for efficient temperature regulation in electric furnaces. The proposed QIO-RPIDD^2 framework was meticulously designed to address the limitations of traditional and advanced PID-based control systems by providing precise and adaptive parameter tuning for complex dynamic systems. Comparative analyses demonstrated that the QIO-RPIDD^2 outperformed well-established metaheuristic algorithms, including FLA, RSA, PSO, and DE, in key performance metrics such as rise time, settling time, overshoot, and steady-state error. Statistical evaluation, convergence analysis, and frequency response assessments further substantiated the superior performance of the QIO in optimizing the RPIDD^2 controller. The proposed method also exhibited exceptional consistency and reliability in handling variable and random temperature profiles, making it a robust solution for industrial temperature control applications. The findings of this study underline the potential of the QIO-RPIDD^2 controller as a significant advancement in industrial control systems, particularly for electric furnace operations requiring high precision and adaptability. By achieving faster transient responses, reduced overshoot, and minimal steady-state error, the proposed approach offers a substantial improvement over conventional control methods, enabling enhanced energy efficiency and process stability.

Future work may explore several avenues to further enhance the utility and applicability of the proposed method. First, real-time implementation of the QIO-RPIDD^2 framework on physical electric furnace systems may be conducted to validate its practicality and robustness in real-world environments. Second, the integration of QIO with advanced machine learning techniques, such as deep reinforcement learning, may be investigated to enable adaptive control in highly non-linear and time-varying systems. Third, the scalability of the QIO may be assessed by applying it to other multi-objective optimization problems, including renewable energy systems and smart manufacturing processes. Lastly, efforts may focus on developing hybrid optimization techniques that combine the strengths of QIO with other emerging metaheuristic algorithms to further enhance convergence speed and global search capabilities.

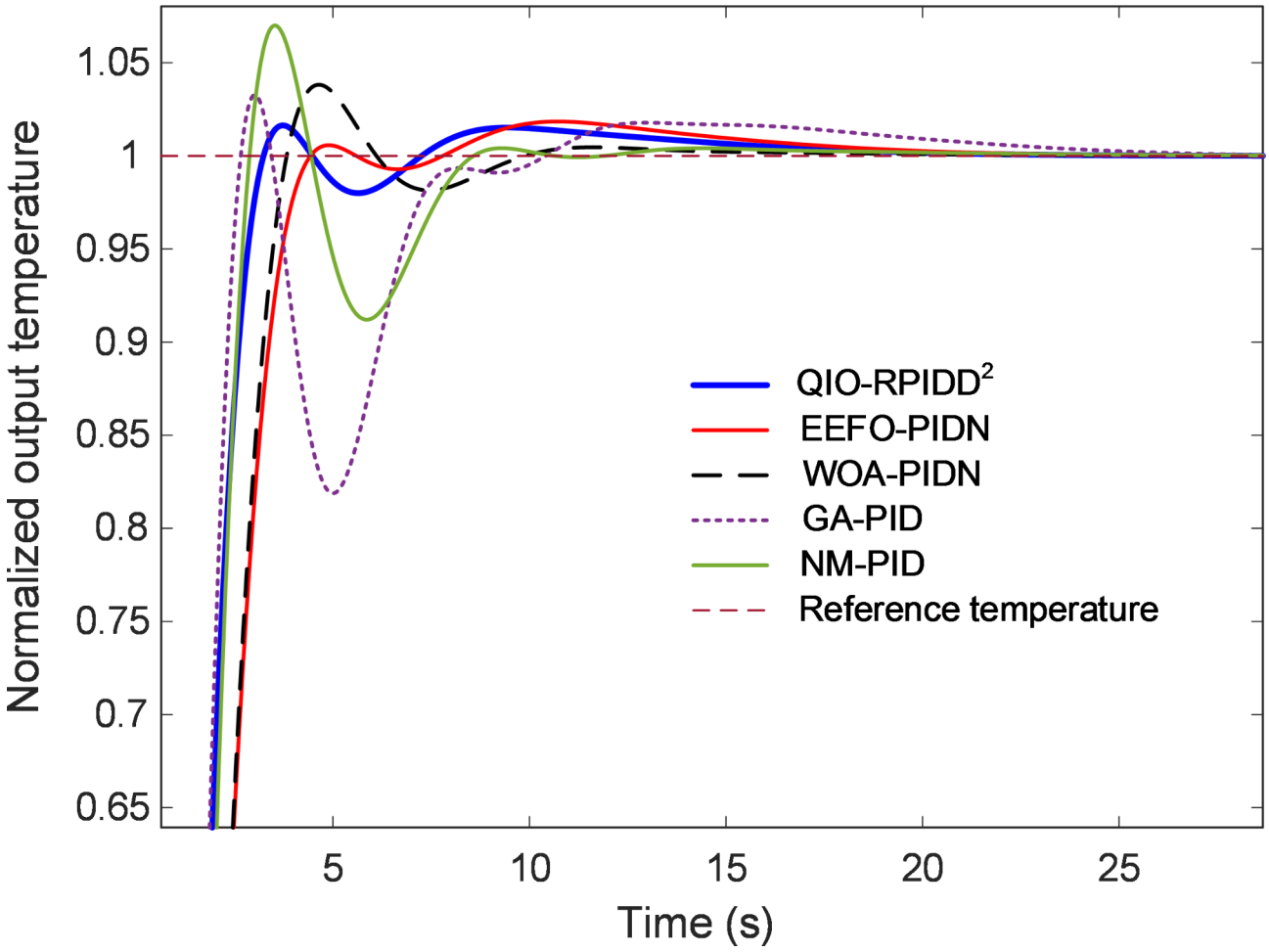


Fig. 10. Enlarged view of (Fig. 9).

Control methods	t_{rise} (s)	t_{set} (s)	O_{shoot} (%)	S_{error} (%)
QIO-RPIDD^2	1.5367	3.0340	1.6355	4.5186E − 12
EEFO-PIDN	2.0330	4.0212	1.8421	6.8168E − 12
WOA-PIDN	1.8674	5.4821	3.8198	3.0287E − 11
GA-PID	1.1378	7.3185	3.2725	1.6148E − 07
NM-PID	1.3047	7.7546	7.0026	1.0345E − 10

Table 7. Comparison of transient response specifications for proposed QIO-RPIDD^2 and other reported control methods.

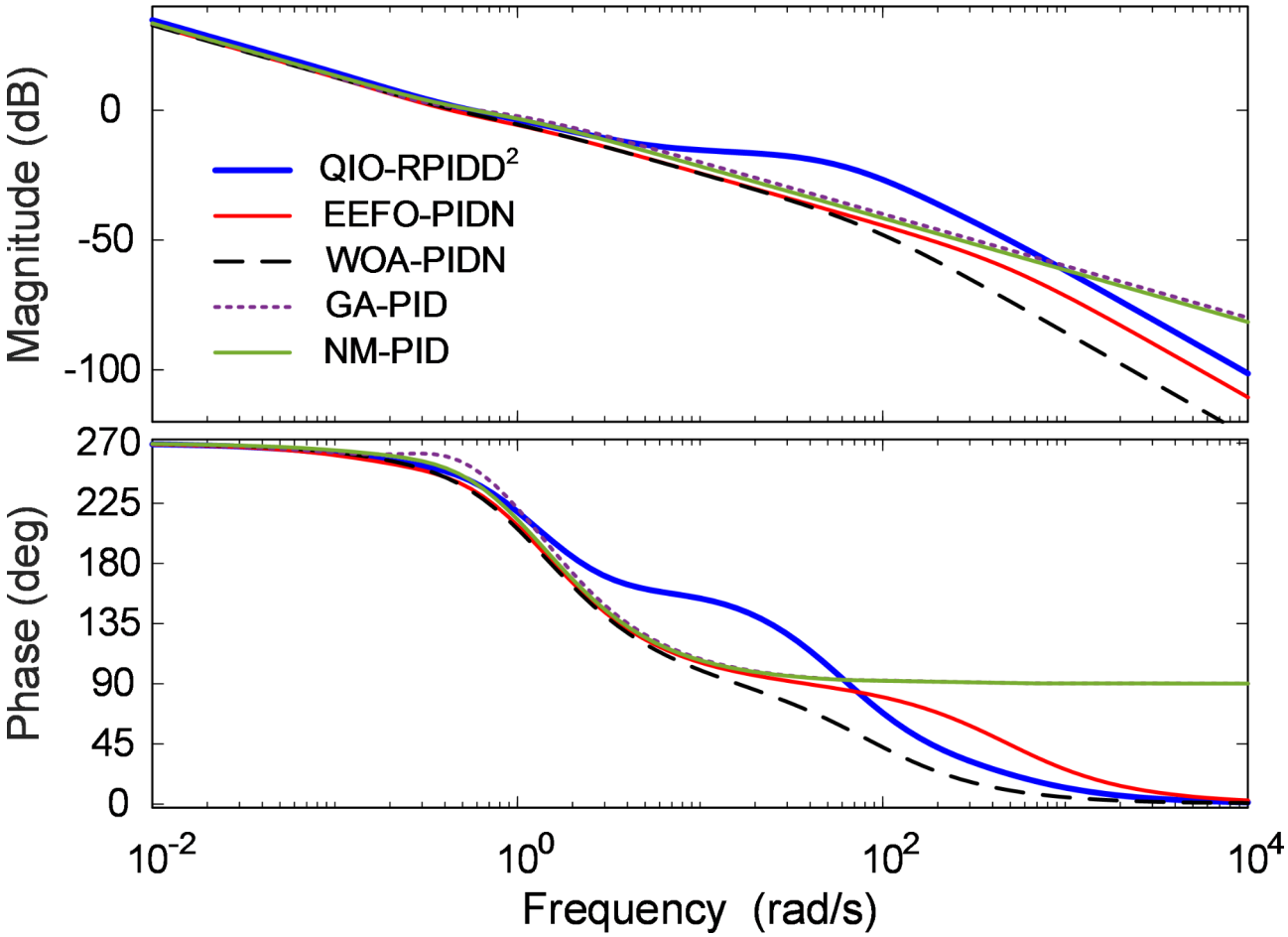


Fig. 11. Bode diagrams of open-loop system for proposed QIO-RPIDD^2 and other reported control methods.

Control methods	P_{margin} (°)	G_{margin} (dB)	B_{width} (rad/s)
QIO-RPIDD^2	61.1612	8.9420	1.8326
EEFO-PIDN	63.0627	8.9281	1.3027
WOA-PIDN	60.4229	8.5523	1.3379
GA-PID	68.9974	5.8858	2.2322
NM-PID	60.3659	6.7057	1.8708

Table 8. Comparison of frequency response specifications for proposed QIO-RPIDD^2 and other reported control methods.

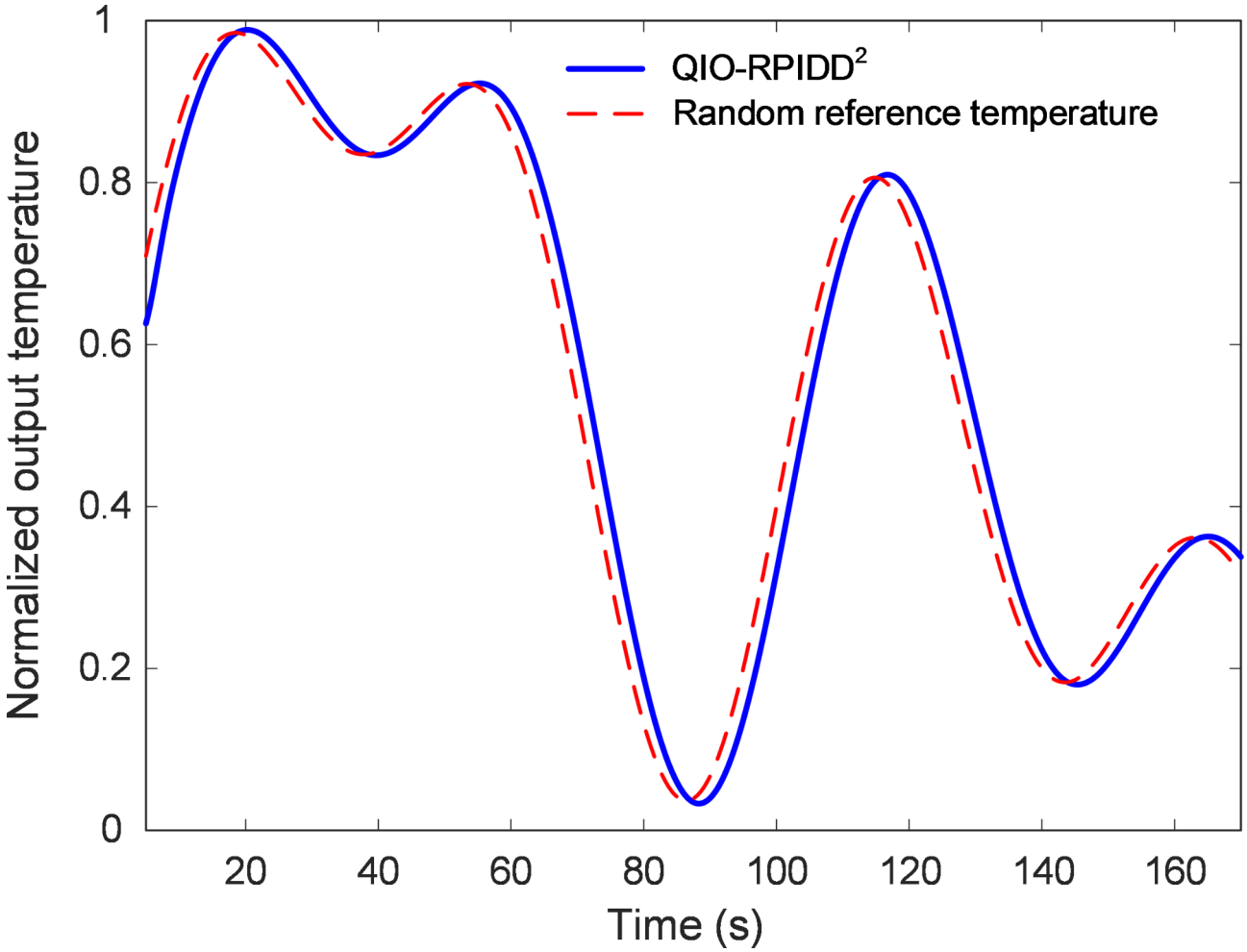


Fig. 12. Closed-loop step response of proposed QIO-RPIDD^2 controlled system for random reference temperature.

Data availability

The datasets used and/or analyzed during the current study available from the corresponding author on reasonable request.

Received: 22 November 2024; Accepted: 19 December 2024
Published online: 02 January 2025

References

1. Gani, M. M., Islam, M. S. & Ullah, M. A. Optimal PID tuning for controlling the temperature of electric furnace by genetic algorithm. *SN Appl. Sci.* **1**, 880 (2019).
2. Hussein, M. M. et al. Modern temperature control of electric furnace in industrial applications based on modified optimization technique. *Energies (Basel)* **15**, 8474 (2022).
3. Almasoudi, F. M., Magdy, G., Bakeer, A., Alatawi, K. S. S. & Rihan, M. A new load frequency control technique for Hybrid Maritime microgrids: sophisticated structure of fractional-order PIDA controller. *Fractal Fract.* **7**, 435 (2023).
4. Huba, M., Bistak, P., Brieznik, J., Vrancic, D. Constrained series PI, PID and PIDA controller design inspired by Ziegler–Nichols. *Power Electron. Drives* **9**, 331–346 (2024).
5. Jamil, A. A., Tu, W. F., Ali, S. W., Terriche, Y. & Guerrero, J. M. Fractional-order PID controllers for temperature control: a review. *Energies (Basel)* **15**, 3800 (2022).
6. Izci, D. & Ekinci, S. An improved RUN optimizer based real PID plus second-order derivative controller design as a novel method to enhance transient response and robustness of an automatic voltage regulator. *e-Prime Adv. Electr. Eng. Electron. Energy* **2**, 100071 (2022).
7. Ekinci, S., Izci, D. & Kayri, M. An effective controller design approach for magnetic levitation system using novel improved manta ray foraging optimization. *Arab. J. Sci. Eng.* **47**, 9673–9694 (2022).
8. Goodwin, G. C., Middleton, R. H., Seron, M. M. & Campos, B. Application of nonlinear model predictive control to an industrial induction heating furnace. *Annu. Rev. Control* **37**, 271–277 (2013).
9. Carlsson, L. S., Samuelsson, P. B. & Jönsson, P. G. Predicting the electrical energy consumption of electric arc furnaces using statistical modeling. *Met. (Basel)* **9**, 959 (2019).
10. Li, H., Li, R. & Wu, F. A. New Control performance evaluation based on LQG Benchmark for the heating furnace temperature control system. *Processes* **8**, 1428 (2020).

11. Dequan, S., Guili, G., Zhiwei, G. & Peng, X. Application of expert fuzzy PID method for temperature control of heating furnace. *Proc. Eng.* **29**, 257–261 (2012).
12. Cao, J., Ye, Q. & Li, P. Resistance furnace temperature control system based on OPC and MATLAB. *Meas. Control* **48**, 60–64 (2015).
13. Xu, W., Zhang, J. & Zhang, R. Application of multi-model switching predictive functional control on the temperature system of an electric heating furnace. *ISA Trans.* **68**, 287–292 (2017).
14. Meng, J. et al. Design of vacuum annealing furnace temperature control system based on GA-Fuzzy-PID algorithm. *PLoS One* **18**, e0293823 (2023).
15. Garai, S., Dutta, R., Dey, S., Parui, S. & Chakrabarty, P. Cascade IMC controller design for heating furnace temperature control. *Int. J. Eng. Manag. Res. (IJEMR)* **6**, 289–297 (2016).
16. Zhang, L. & Tan, B. Analysis on temperature control of tubular furnace based on fuzzy control. *Sens. Transducers* **155**, 205 (2013).
17. Hou, X. G. & Wang, C. L. Induction heating furnace temperature control based on the fuzzy PID. *Appl. Mech. Mater.* **217–219**, 2463–2466 (2012).
18. Kumar, V. B., Rao, K. S., Charan, G. & Pavan Kumar, Y. V. Industrial Heating Furnace Temperature Control System Design Through Fuzzy-PID Controller. in *2021 IEEE International IOT, Electronics and Mechatronics Conference (IEMTRONICS)* 1–6 https://doi.org/10.1109/IEMTRONICS52119.2021.9422491 (2021).
19. Ghiormez, L., Panoiu, M. & Panoiu, C. Fuzzy logic controller for power control of an electric arc furnace. *Mathematics* **12**, 3445 (2024).
20. Khan, M., Ahmad, I., Ahsan, M., Kano, M. & Caliskan, H. Prediction of optimum operating conditions of a furnace under uncertainty: an integrated framework of artificial neural network and genetic algorithm. *Fuel* **330**, 125563 (2022).
21. Daraz, A., Malik, S. A., Saleem, T. & Bhati, S. A. Ziegler Nichols based integral proportional controller for superheated steam temperature control system. *Int. J. Electr. Comput. Energet. Electron. Commun. Eng.* **11**, 516–520 (2017).
22. Tian, H., Tang, J. & Wang, T. Furnace temperature model predictive control based on particle swarm rolling optimization for municipal solid waste incineration. *Sustainability* **16**, 7670 (2024).
23. López-Palenzuela, A. et al. Temperature control in Solar furnaces using nonlinear PID-based control approaches. *Int. J. Control Autom. Syst.* **22**, 2419–2427 (2024).
24. Sheng, T., Luo, H. & Wu, M. Design and simulation of a multi-channel biomass hot air furnace with an intelligent temperature control system. *Agriculture* **14**, 419 (2024).
25. Surus, R., Strzałkowski, K. & Tarczewski, T. High-performance temperature control system for resistance furnace annealing and crystal growth of semiconductor compounds. *Results Eng.* **17**, 100863 (2023).
26. Wang, T. et al. Intelligent optimal control of furnace temperature for the municipal solid waste incineration process using multi-loop controller and particle swarm optimization. *Expert Syst. Appl.* **257**, 125015 (2024).
27. Gabirondo-López, J., Arredondo, I. & Igartua, J. M. Temperature Control of Nonlinear Uncertain Systems via Model-Free Cascaded Controller: application to an Infrared Emissometer. *IEEE Trans. Control Syst. Technol.* 1–0 https://doi.org/10.1109/TCST.2024.3464111 (2024).
28. Chen, C. J., Liao, Y. C. & Chou, F. I. Optimal design of the cascade controller for reheating furnace by taguchi method. *IEEE Access* **12**, 39728–39736 (2024).
29. Beccaro, W., Ramos, C. A. S. & Duarte, S. X. Optimizing semiconductor processing open tube furnace performance: comparative analysis of PI and Mamdani fuzzy-PI controllers. *J. Intell. Manuf.* **34**, 3015–3024 (2023).
30. Zhang, X., Cao, Z., Wang, S., Yao, L. & Yu, H. High-speed temperature control method for MEMS thermal gravimetric analyzer based on dual fuzzy PID control. *Micromach. (Basel)* **14**, 929 (2023).
31. Jiang, W. & Jiang, X. Design of an intelligent temperature control system based on the fuzzy self-tuning PID. *Proc. Eng.* **43**, 307–311 (2012).
32. Liu, L., Xue, D. & Zhang, S. General type industrial temperature system control based on fuzzy fractional-order PID controller. *Complex. Intell. Syst.* **9**, 2585–2597 (2023).
33. Yerolla, R., Besta, C. S. & P, S. & Advanced temperature control in ethanol fermentation using a PSO-PID controller with split-range control strategy. *Prep Biochem. Biotechnol.* 1–13 https://doi.org/10.1080/10826068.2024.2381761 (2024).
34. Golbahar Haghighi, M. R., Eghtesad, M., Necsulescu, D. S. & Malekzadeh, P. Temperature control of functionally graded plates using a feedforward–feedback controller based on the inverse solution and proportional-derivative controller. *Energy Convers. Manag.* **51**, 140–146 (2010).
35. Pringsakul, N. & Puangdownreong, D. Mofpa-based pida controller design optimization for electric furnace temperature control system. *Int. J. Innovat. Comput. Inform. Control* **16**, 1863–1876 (2020).
36. Wang, C., Xu, M. & Yan, B. WOA-Based Fuzzy Self-Tuning PID Evaporative Source Temperature Control. in *International Symposium on Robotics, Artificial Intelligence, and Information Engineering (RAIIE 2022)* (ed. Debayle, J.) 19 https://doi.org/10.1117/12.2658354 (SPIE, 2022).
37. Alzakari, S. A., Izci, D., Ekinci, S., Alhussan, A. A. & Hashim, F. A. A new control scheme for temperature adjustment of electric furnaces using a novel modified electric eel foraging optimizer. *AIMS Math.* **9**, 13410–13438 (2024).
38. Zhang, R., Zou, Q., Cao, Z. & Gao, F. Design of fractional order modeling based extended non-minimal state space MPC for temperature in an industrial electric heating furnace. *J. Process. Control* **56**, 13–22 (2017).
39. Sinlapakun, V. & Assawinchaichote, W. Optimized PID Controller Design for Electric Furnace Temperature Systems with Nelder Mead Algorithm. in *12th International Conference on Electrical Engineering/Electronics, Computer, Telecommunications and Information Technology (ECTI-CON)* 1–4 https://doi.org/10.1109/ECTICon.2015.7206925 (IEEE, 2015).
40. Veinović, S., Stojić, D. & Ivanović, L. Optimized PIDD2 controller for AVR systems regarding robustness. *Int. J. Electr. Power Energy Syst.* **145**, 108646 (2023).
41. Kumar, M. & Hote, Y. V. Robust PIDD2 controller design for perturbed load frequency control of an interconnected time-delayed power systems. *IEEE Trans. Control Syst. Technol.* **29**, 2662–2669 (2021).
42. Li, Y., Bi, J., Han, W. & Tan, W. Tuning of PID/PIDD2 controllers for integrating processes with robustness specification. *ISA Trans.* https://doi.org/10.1016/j.isatra.2023.05.015 (2023).
43. Li, Y., Tan, W. & Yu, M. Tuning rules of filtered PID/PIDD 2 controller for integrating processes with measurement noise. *Int. J. Syst. Sci.* **55**, 467–481 (2024).
44. Hu, X., Tan, W. & Hou, G. PIDD2 control of large wind turbines' Pitch angle. *Energies (Basel)* **16**, 5096 (2023).
45. Meidani, K. & Mirjalili, S. Barati Farimani, A. Online metaheuristic algorithm selection. *Expert Syst. Appl.* **201**, 117058 (2022).
46. Akbari, E. et al. Improved salp swarm optimization algorithm for damping controller design for multimachine power system. *IEEE Access* **10**, 82910–82922 (2022).
47. Khajehzadeh, M. & Eslami, M. Gravitational search algorithm for optimization of retaining structures. *Indian J. Sci. Technol.* **5**, 1821–1827 (2012).
48. Boroumandfar, G., Khajehzadeh, A., Eslami, M. & Syah, R. B. Y. Information gap decision theory with risk aversion strategy for robust planning of hybrid photovoltaic/wind/battery storage system in distribution networks considering uncertainty. *Energy* **278**, 127778 (2023).
49. Zhao, W. et al. Quadratic interpolation optimization (QIO): a new optimization algorithm based on generalized quadratic interpolation and its applications to real-world engineering problems. *Comput. Methods Appl. Mech. Eng.* **417**, 116446 (2023).

50. Ghasemi, M. et al. Flood algorithm (FLA): an efficient inspired meta-heuristic for engineering optimization. *J. Supercomput.* **80**, 22913–23017 (2024).
51. Abualigah, L., Elaziz, M. A., Sumari, P., Geem, Z. W. & Gandomi, A. H. Reptile search algorithm (RSA): a nature-inspired meta-heuristic optimizer. *Expert Syst. Appl.* 116158 https://doi.org/10.1016/j.eswa.2021.116158 (2021).
52. Wang, D., Tan, D. & Liu, L. Particle swarm optimization algorithm: an overview. *Soft Comput.* **22**, 387–408 (2018).
53. Storn, R. & Price, K. Differential evolution—A simple and efficient heuristic for global optimization over continuous spaces. *J. Glob. Optim.* **11**, 341–359 (1997).
54. Izci, D., Ekinci, S. & Hussien, A. G. An elite approach to re-design Aquila optimizer for efficient AFR system control. *PLoS One* **18**, e0291788 (2023).

Author contributions

Serdar Ekinci, Davut Izci, Veysel Gider: Conceptualization, Methodology, Software, Visualization, Investigation, Writing—Original draft preparation. Laith Abualigah: Data curation, Validation, Supervision, Resources, Writing—Review & Editing. Mohit Bajaj, Ievgen Zaitsev: Project administration, Supervision, Resources, Writing—Review & Editing.

Declarations

Competing interests

The authors declare no competing interests.

Additional information

Correspondence and requests for materials should be addressed to M.B. or I.Z.

Reprints and permissions information is available at www.nature.com/reprints.

Publisher's note Springer Nature remains neutral with regard to jurisdictional claims in published maps and institutional affiliations.

Open Access This article is licensed under a Creative Commons Attribution-NonCommercial-NoDerivatives 4.0 International License, which permits any non-commercial use, sharing, distribution and reproduction in any medium or format, as long as you give appropriate credit to the original author(s) and the source, provide a link to the Creative Commons licence, and indicate if you modified the licensed material. You do not have permission under this licence to share adapted material derived from this article or parts of it. The images or other third party material in this article are included in the article's Creative Commons licence, unless indicated otherwise in a credit line to the material. If material is not included in the article's Creative Commons licence and your intended use is not permitted by statutory regulation or exceeds the permitted use, you will need to obtain permission directly from the copyright holder. To view a copy of this licence, visit http://creativecommons.org/licenses/by-nc-nd/4.0/.

© The Author(s) 2024